

## Supplementary information

### 1. Experimental details

#### 1.1. Preparation of alloy and composites

The starting materials are in powder form and were thoroughly mixed using effective powder mixing procedures to obtain homogenous admixed powders. Subsequently, the admixed powder was transferred to the spark plasma sintering machine for consolidation. The microstructure, mechanical, and tribological properties of the developed composites were tested thereafter.

##### 1.1.1. Materials and process

The gas-atomized AZ91D Mg-based alloy (matrix starting powder) with 99.7% purity and spherical particle size ranges between 15 and 53  $\mu\text{m}$  was obtained from Dome metal in China. Wear Tech Ltd, South Africa, supplied the Ni powder with 99.5% purity and spherical particle sizes between 0.5 to 3  $\mu\text{m}$ , while graphene nanoplatelets (GNPs) were obtained from Sigma-Aldrich, South Africa. The GNPs have a surface area between 15-30  $\text{m}^2/\text{g}$ , an average diameter of 5  $\mu\text{m}$  and an average thickness of 15 nm, as obtained from the manufacturer. The percentage of Ni constituent is fixed at 1.5 wt% [1, 2], while the GNP constituent varies from 0 to 2 wt% with reference to the AZ91D Mg alloy matrix. A blending technique using a tubular mixer was employed. In addition to the measured powders placed in a container, tungsten balls are placed at a 10:1 ball-to-powder ratio to ensure complete mixing without a process control agent. The tubular mixer has a holding chamber that moves in a 3D direction, combining rotational and translational motion and is operated for 12 hours at a speed of 110 rpm. At the completion of the process, the admixed powders were conveyed to a planetary ball milling machine (PM 400) to complete the systematic mechanical mixing. An ethanol solution (process control agent) and tungsten balls (10:1 ball-to-powder ratio) were added to the admixed powder to promote uniform mixing. The airtight

mixing process is conducted for 5 hours at a mixing speed of 200 rpm [2]. Also, the wet powder, after mixing, is conveyed to a LAB conco vacuum dryer operated at 70 °C for 6 hours to remove the ethanol solution in the admixed powders. The mode of operation of the milling machine and its description are documented in our previous study [3]. To prevent an agglomerate from forming within the body of the powder after drying, the powders with the tungsten balls are taken to the tubular mixer operated at a low rotating speed of 49 rpm for 1 hour. A 5.43 g quantity of AZ91D-Ni alloy and AZ91D-Ni-GNPs composite admixed powders sufficient to produce a 20 mm x 10 mm disc sample size is measured and transferred into a  $\varnothing$  20 mm graphite die mould.

### **1.1.2. Spark plasma sintering of Mg-based AZ91D-Ni alloy and AZ91D-Ni-GNPs composites.**

Subsequently, the admixed powder placed in the graphite die is transferred into the heating chamber of the SPS system (Model HHPD-23, FCT Germany) for sintering and consolidation processes. The powders were sintered in a vacuum atmosphere maintained at 0.5 mbar utilizing an argon gas controlling agent to remove oxygen contamination and afterwards, using the following sintering parameters: a pressure of 50 Mpa, a heating rate of 100 °C/min, holding time of 5 min and a sintering temperature of 500 °C. A 2 mm thick graphite foil is applied to line the internal surface of the graphite die and punches (the surface that made contact with the admixed powder) to ensure easy removal of the sintered sample and aid heat distribution during the sintering cycle. The theoretical density of the mixed powder is calculated to be 1.76 g/cm<sup>3</sup> for the composites and 1.78 g/cm<sup>3</sup> for the alloy. A pyrometer is connected to the upper electrode and upper graphite tooling to measure the temperature of the alloy/composites during fabrication. The machine is turned off at the end of the sintering process (when the set temperature and holding time have been attained). The sample is left to cool in the SPS chamber and afterwards removed for sandblasting to eliminate the graphite foils and other impurities attached to its surface during sintering. The

sintering parameters employed assist in promoting the good formation of strong metallurgical bonding due to effective contact between the particles of the powders. The schematic illustration of the manufacturing processes of AZ91D-Ni alloy and AZ91D-Ni-GNPs Mg-based composites is presented in **Fig. 1**.

### **1.1.3. Metallographic preparation of the sintered Mg-based AZ91D-Ni alloy and AZ91D-Ni-GNPs composites samples**

The sintered samples were sectioned into small pieces before microstructure analysis using an electrical discharge wire-cutting machine. Afterwards, they were ground using silicon carbide (SiC) papers with different grit sizes ranging from p320 to 4000. The samples were mechanically polished using Aker Allegra 3 plate with 9, 6, 3 and 1  $\mu\text{m}$  diamond suspension paste (diamaxx: mono), followed by fused silica suspension for the final polishing stage. Lastly, ethanol is used to rinse the mirror-like surface of each sample. The samples were etched in an acidic solution of acetic acid (5 ml), picric acid (3 ml), distilled water (10 ml), and ethanol (50 ml) prepared.

### **1.2. Characterization of the sintered Mg-based AZ91D-Ni alloy and AZ91D-Ni-GNPs composites**

The bulk relative density of the sintered AZ91D-Ni alloy and AZ91D-Ni-GNPs composites was measured following the Archimedes principle and according to the ASTM C373-88 standard [4]. An electronic densimeter with an accuracy of  $\pm 0.0001\text{g}$  is employed for the measurement. At first, the sintered components were weighed in the air and then immersed in distilled water to evaluate the relative density following Archimedes' principle. Seven relative density measurements were conducted for each sample, with the average calculated and taken as the actual relative density value. This is converted to a percentage by dividing the bulk relative density values

with the theoretical calculated density multiplied by a hundred for each sample using the mixture rule [5]. The morphology of the as-received powders (AZ91D Mg alloy, Ni, GNPs), sintered alloy/composites (microstructure and elemental dispersion) and worn surface were observed using an optical microscope (Falcon 500 series) and Zeiss Ultra Plus 55 field emission scanning electron microscope. It is incorporated with energy-dispersive X-ray (EDS) spectra operated at 1.0 kV. The admixed powders were observed using a JEOL-2100F high-resolution transmission electron microscope (HRTEM FEI Tecnai-F30) at 200 kV accelerating voltage. The various phases formed in the sintered composites were identified using a PANalytical Empyrean X-ray diffractometry at a scanning rate of 0.02 °/sec with CuK $\alpha$  radiation ( $\lambda = 0.154$  nm) at 50 kV and 30 mA over the angular range of 10-90°. A T64000 micro-Raman spectrometer (HORIBA Scientific, Jobin Yvon Technology) is used to characterize the sintered components operating at 514 nm laser wavelength and 120 s spectral acquisition time. The data of the Raman spectra were obtained on 8 different spots to ensure data accuracy, and the Raman shifts of the D and G bands were calibrated following ASTM E1840-96 standard [6]. The optical micrographs displaying different grain shapes, sizes, and boundaries were characterized by assessing the area of the grains in each direction to quantify the grain size distribution. An ImageJ graphics software is employed in this regard.

### **1.3. Microhardness testing**

The microhardness value of the sintered alloy and composite samples is evaluated using an automated digital Vickers microhardness tester (Future-tech). A load of 500 gf (5N) and a dwell time of 15 s were used for the polished test samples. The microhardness testing is conducted ten times at different spots to ensure that all features are captured. Thus, the actual microhardness value used for each sample in this study is the arithmetic mean of the ten consecutive indentations.

#### **1.4. NanoIndentation testing**

The mounted and polished (mirror-like surface) samples were placed in the motorized stage of the nanoindenter (Anton Paar, TTX-NHT<sup>3</sup>) tester. Afterwards, the nanomechanical properties of the sintered AZ91D-Ni alloy and AZ91D-Ni-GNPs composites were conducted following the ASTM E2546-15 standard. A load of 100 mN, a loading time and unloading time of 25 s, and a holding time of 10 s are the operating parameters used for the analysis of each sample. An average of six nanoindentation tests are performed and presented in this study. The nanoindentation tester is equipped with a diamond Berkovich pyramid indenter (three-sided). The Oliver & Pharr method is used to calculate the elastic modulus (Mpa) and nanohardness (GPa) of the sintered components via appropriate equations, as demonstrated by Okoro A.M. et al.[7] and Dada, M. et al.[8].

#### **1.5. Wear analysis**

The dry sliding wear performance of the sintered AZ91D-Ni alloy and AZ91D-Ni-GNPs composites were examined at room temperature (~24°C) utilizing a tribometer (Anton Paar, TRB3) machine in accordance with ASTM G99-95 standard. The wear testing is conducted using a pin-on-disc dry-sliding rotating part equipped with a wear and friction monitor system. The wear analysis is performed using a speed of 300 rpm and a load of 10 N for 15 min. A stainless-steel pin with a 1 mm tip diameter and 0.03 mm roughness (Ra) counter body is used for the analysis in the absence of any lubricating medium. The design of the system requires that the pin is positioned stationary over the topmost surface of the test sample and the test piece pre-fixed on an axially rotating disk that unidirectionally slides during experimentation. The variation in the coefficient of friction and wear rate with respect to the sliding time for the sintered Mg-based components was estimated and recorded. The wear rate is directly obtained using a profilometer (Surtronic

S128) attached to the tribometer. This process determined the wear rate by measuring the profiles of the wear tracks caused by plastic deformation.

## Result

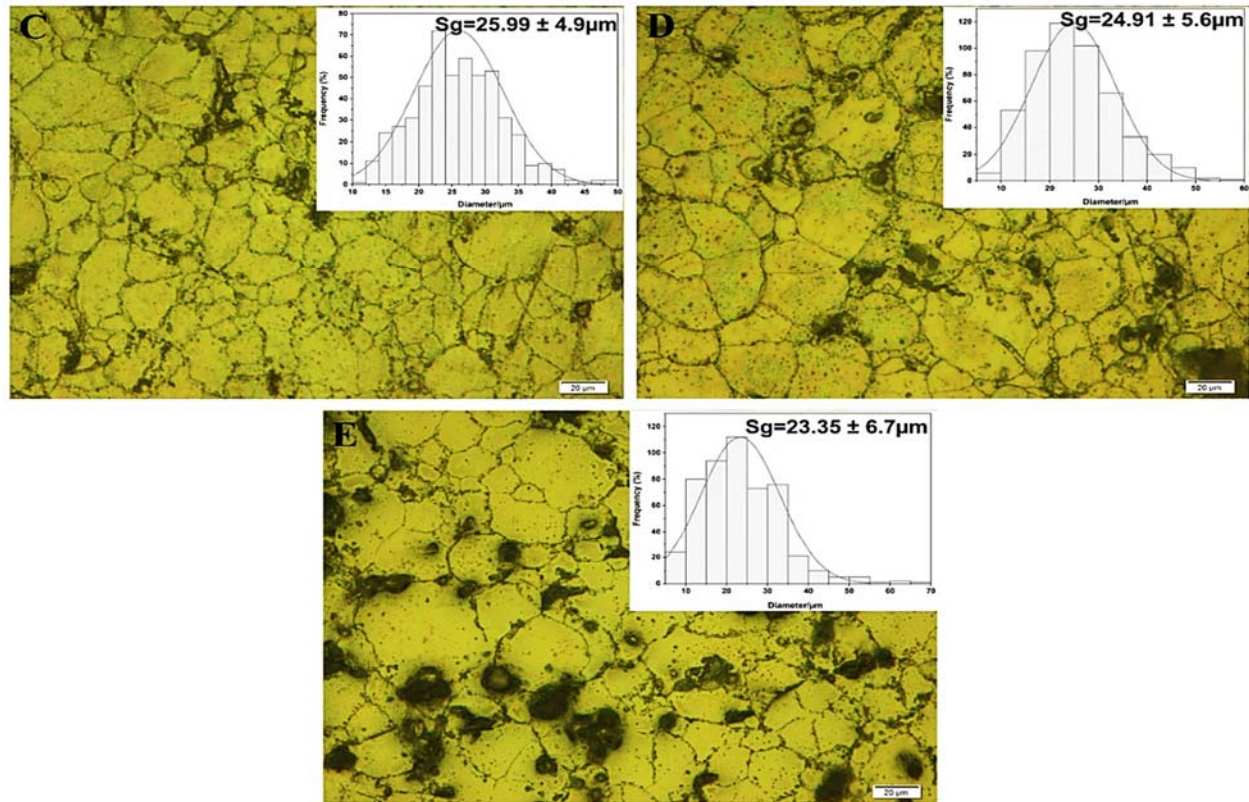


**Fig. 3S.** Optical microstructures and grain size distribution of sintered Mg-based AZ91D-Ni alloy and AZ91D-Ni-GNPs composites (a) 0 wt% GNPs, (b) 0.5 wt% GNPs, (c) 1 wt% GNPs, (d) 1.5 wt% GNPs, and (e) 2 wt% GNPs.

## Reference

- [1] Olalekan, Ogunlakin Nasirudeen, M. Abdul Samad, Syed Fida Hassan, and Muhammad Mohamed Ibrahim Elhady. Tribological evaluations of spark plasma sintered Mg–Ni composite. *Tribol. - Mater. Surf. Interfaces* 2022;16(2):110-118

- [2] Hassan, S. Fida, O. O. Nasirudeen, N. Al-Aqeeli, N. Saheb, F. Patel, and M. M. A. Baig. Magnesium–nickel composite: Preparation, microstructure and mechanical properties. *J. Alloys Compd* 2015;646: 333-338.
- [3] Ogunbiyi, Olugbenga, Rotimi Sadiku, Oluwagbenga Adesina, Olanrewaju Seun Adesina, Smith Salifu, and Juwon Fayomi. Microstructure and mechanical properties of spark plasma-sintered graphene-reinforced Inconel 738 low carbon superalloy. *Metall. Mater. Trans. A* 2022;53:299-313.O.
- [4] Ogunbiyi, O. F., E. R. Sadiku, T. Jamiru, O. T. Adesina, and L. W. Beneke. Spark plasma sintering of Inconel 738LC: densification and microstructural characteristics. *Mater. Res. Express* 2019;6(10):1065-8.
- [5] Ogunbiyi, Olugbenga, Tamba Jamiru, Rotimi Sadiku, Oluwagbenga Adesina, Olanrewaju Seun Adesina, and Emmanuel Olorundaisi. Influence of Nickel powder particle size on the microstructure and densification of spark plasma sintered Nickel-based superalloy. *Int. J. Eng. Res. Africa* 2021;53:1-19.
- [6] Wall M.. The Raman spectroscopy of graphene and the determination of layer thickness. *Thermo Sci* 2011;5:1-5.
- [7] Okoro, Avwersuoghene Moses, Ronald Machaka, Senzeni Siphon Lephuthing, Samuel Ranti Oke, Mary Ajimegoh Awotunde, and Peter Apata Olubambi. "Nanoindentation studies of the mechanical behaviours of spark plasma sintered multiwall carbon nanotubes reinforced Ti6Al4V nanocomposites." *Materials Science and Engineering: A* 765 (2019): 138320.

- [8] Dada, M., P. Popoola, N. Mathe, S. Adeosun, and S. Pityana. Investigating the elastic modulus and hardness properties of a high entropy alloy coating using nanoindentation. *Int. J. lightweight mater. manuf* 2021;4(3):339-345.